Appl Phys B (2009) 95: 367–373
DOI 10.1007/s00340-009-3362-x

**Applied Physics B**
**Lasers and Optics**

# Effect of Cd and Pb impurities on the optical properties of fresh evaporated amorphous $(As_2Se_3)_{90}Ge_{10}$ thin films

**P. Sharma · S.C. Katyal**

Received: 13 October 2008 / Revised version: 2 December 2008 / Published online: 23 January 2009


**Abstract** Transmission spectra (400–1500 nm) of thermally evaporated amorphous $[(As_2Se_3)_{90}Ge_{10}]_{95}M_5$ thin films have been analyzed to study the effect of impurities (M = Cd and Pb) on their optical properties. The refractive index increases with addition of metal impurities. The dispersion of refractive index has been studied using Wemple–DiDomenico single oscillator model. The optical gap has been estimated using Tauc's extrapolation and was found to decrease with the addition of metal impurities from 1.46 to 1.36 eV (Cd) and 1.41 eV (Pb) with an uncertainty of ±0.01 eV. The change in optical properties with metal impurities has been explained on the basis of density, polarizability and bond energy of the system.

**PACS** 78.55.Qr · 77.84.Bw · 78.20.Ci

## 1 Introduction

Chalcogenide glasses are a recognized group of inorganic glassy materials, which always contain one or more of the chalcogen elements S, Se or Te. They are generally less robust and weaker-bonded materials than oxide glasses. However, they have superior properties that vary with the change in chemical composition and can be applied in devices. Chalcogenide glasses have easy fabrication and processing, good chemical durability, high photosensitivity, low phonon energy, and second or third order optical non-linearity due to their high refractive index. So chalcogenide glasses have a wide variety in photonic applications, such as optical recording devices, optical amplifiers, ultrafast optical switches, infrared lasers, and infrared transmitting optical fibers [1–4].

The optical properties of the amorphous As–Se–Ge system have been extensively studied [5–7] because of the fact that Ge, As and Se are the elements of same period in groups IV–VI and bring about the covalent character of the interaction between their atoms. This results in a broad glass formation region in the As–Se–Ge system [8] among all investigated three-component chalcogenide systems. Generally, the undoped chalcogenide glasses show low values of electrical conductivity, which could mean a serious limitation to their technological application. Certain additives are used to improve these properties. It was believed earlier that impurities have little effect on the properties of amorphous semiconductors as each impurity atom can satisfy its valence requirement by adjusting its nearest neighbor environment. However, Fritzsche et al. [9] have shown that the effect of charged additives in lone-pair semiconductors depends on whether the charged additives equilibrate or not with a valence alternation defect.

In a recent research scenario, it has been observed that chalcogenide glasses are sensitive to composition, impurities and deposition parameters like thickness, substrate type and substrate temperature [10–15]. Recent experiments [11, 15] reveal that the addition of impurities, like Bi and Pb, have produced a remarkable change in the optical and electrical properties of chalcogenide glasses. It is conjectured that with the addition of metal impurities in the $(As_2Se_3)_{90}Ge_{10}$ system there may be remarkable a change in their optical properties. Thus, a thorough study of optical properties is considered crucial to have a better understanding of the system.

P. Sharma (✉) · S.C. Katyal
Department of Physics, Jaypee University of Information Technology, Waknaghat, Solan, H.P. 173215, India
e-mail: pks_phy@yahoo.co.in

P. Sharma (✉)
e-mail: pankaj.sharma@juit.ac.in

In the present work, we have reported the effect of metal impurities on the optical properties of $[(As_2Se_3)_{90}Ge_{10}]_{95}M_5$, where M = Cd and Pb, thin films. The optical properties of amorphous thin films have been measured by analyzing their transmission spectra in the spectral range of 400–1500 nm. This analysis was pioneered by Manifacier [16] and extended by Swanepoel [17], and since then has been successfully applied to several chalcogenide glasses [5, 10, 12, 14, 18, 19]. Swanepoel's method has an advantage due to its nondestructive nature and yields the dispersion relation over a large range of wavelength without any prior knowledge of film's thickness. The optical energy gap has been estimated using Tauc's extrapolation method. The dispersion of refractive index has been studied in terms of Wemple–DiDomenico single oscillator model.

## 2 Experimental details

Glasses of $[(As_2Se_3)_{90}Ge_{10}]_{95}M_5$, where M = Cd and Pb, were prepared by the melt quenching technique. Materials (99.999% purity, Sigma-Aldrich) were weighed according to their atomic percentages and sealed in evacuated (at $\sim 10^{-4}$ Pa) quartz ampoules. The weight of each batch of materials was taken as 4 g. The sealed ampoules were kept inside a furnace where the temperature was increased up to 950°C at a heating rate of 3–4°C $\text{min}^{-1}$. The ampoules were frequently rocked for 24 h at the highest temperature to make the melt homogeneous. The quenching was done in ice-cold water. Glasses were obtained by breaking the ampoules. Density of bulk samples was measured using buoyancy method discussed elsewhere [20]. Thin films of $[(As_2Se_3)_{90}Ge_{10}]_{95}M_5$ glasses were deposited on ultrasonically cleaned glass substrates by thermal evaporation at $\sim 10^{-4}$ Pa base pressure. The vacuum evaporation process was carried out in a coating system (HINDHIVAC model 12A4D India). The rate of evaporation ($r$) of deposited thin films under investigation is given in Table 1. The thickness of the deposited films was measured by a thickness monitor (Model DTM-101) and found to be within ±35 nm as estimated later from the fitting of transmission spectra. The amorphous nature of bulk compositions as well as their thin films made for study was examined by the X-ray powder diffraction method using a Philips PW 1710 X-ray diffractometer (the radiation used was CuK$\alpha$). The lack of any sharp peaks indicates the glassy nature of the prepared materials. The compositions of the evaporated samples were measured by an electron microprobe analyzer (JEOL 8600 MX) on different spots (size ≈2 μm) on the sample. The composition of a 2 × 2 $\text{cm}^2$ sample is uniform within the measurement accuracy of ±1–1.5%. The transmission spectra of the thin films in the spectral range 400–1500 nm were obtained using a double beam ultraviolet–visible–near-infrared spectrophotometer (Hitachi-330). The scanning rate of spectrophotometer was set to 2 nm/s. All the measurements reported were taken at 300 K.

## 3 Results

The XRD results are shown in Fig. 1. The lack of Bragg's reflection peaks in the diffractogram confirms the amorphous nature of samples. Optical transmission ($T$) is a very complex function and is strongly dependent on the absorption coefficient ($\alpha$). Figure 2 shows the transmission spectra of amorphous $[(As_{2S}e_3)_{90}Ge_{10}]_{95}M_5$, where M = Cd and Pb, thin films. The refractive index ($n$) and extinction coefficient ($k$) have been calculated using Swanepoel's method [17]. The spectral distribution of refractive index and extinction coefficient is shown in Fig. 3. The values of $n$ at 800 nm are given in Table 1.

The thickness ($d$) of the thin films under investigation has been calculated using [17] and is given in Table 1. The difference in thickness measured from the thickness monitor and calculated using transmission spectra lies within ±35 nm (shows the accuracy of results obtained from spectra).

According to single oscillator model proposed by Wemple–DiDomenico (WDD) model [21, 22], the optical data could be described to an excellent approximation by the following expression

$$n^2(h\nu) = 1 + \frac{E_0 E_d}{E_0^2 - (h\nu)^2}, \tag{1}$$

**Table 1** The values of rate of the deposition ($r$), thickness ($d$), density ($\rho$), refractive index ($n$) at 800 nm, oscillator strength ($E_0$), dispersion energy ($E_d$), static refractive index ($n_0$), and the high frequency dielectric constant ($\varepsilon_\infty$) for $a$-$[(As_2Se_3)_{90}Ge_{10}]_{95}M_5$ (where M = Cd and Pb) thin films

| Composition | $r$ (Å/s) | $d$ (nm) | $\rho$ (g/cc) | $n$ | $E_d$ (eV) | $E_0$ (eV) | $n_0$ | $\varepsilon_\infty$ |
|---|---|---|---|---|---|---|---|---|
| $(As_2Se_3)_{90}Ge_{10}$ | 13.2 | 900 | 5.178 | 2.642 | 15.067 | 3.01 | 2.45 | 6.01 |
| $[(As_2Se_3)_{90}Ge_{10}]_{95}Cd_5$ | 13.0 | 846 | 5.361 | 3.054 | 19.742 | 2.76 | 2.86 | 8.18 |
| $[(As_2Se_3)_{90}Ge_{10}]_{95}Pb_5$ | 13.4 | 929 | 5.536 | 3.496 | 22.723 | 2.84 | 3.00 | 9.00 |

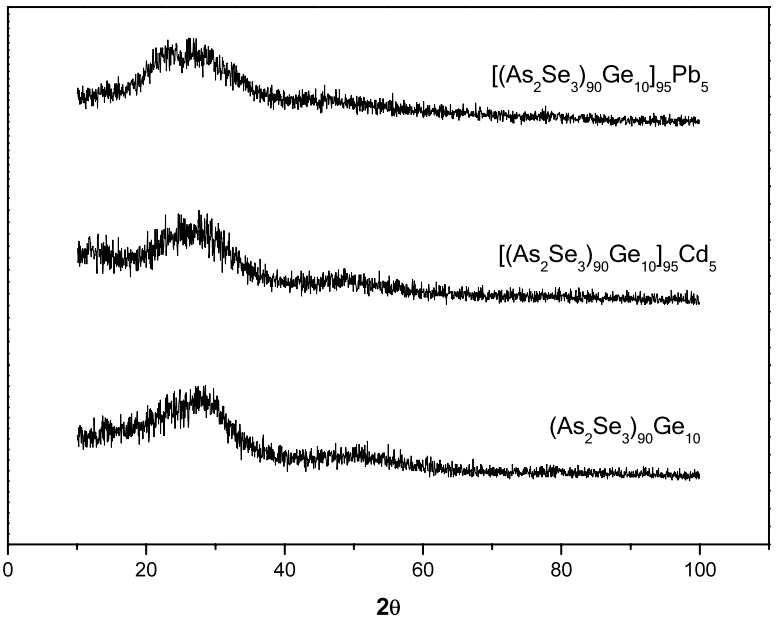


**Fig. 1** XRD patterns for $[(As_2Se_3)_{90}Ge_{10}]_{95}M_5$ (where M = Cd and Pb) thin films

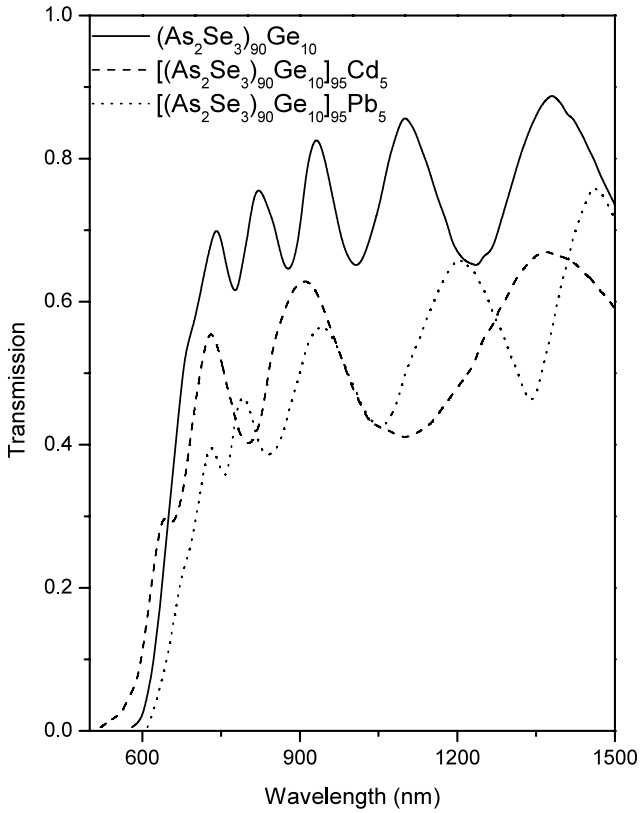


**Fig. 2** Transmission spectra for $a$-$[(As_2Se_3)_{90}Ge_{10}]_{95}M_5$ (where M = Cd and Pb) thin films

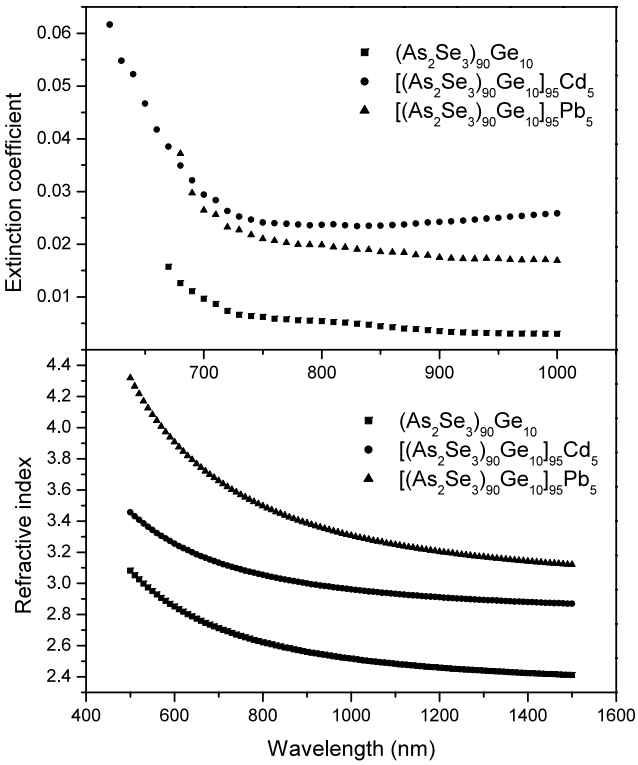


**Fig. 3** A plot of the refractive index ($n$) and extinction coefficient ($k$) versus wavelength (nm) for $a$-$[(As_2Se_3)_{90}Ge_{10}]_{95}M_5$ (where M = Cd and Pb) thin films

where $h\nu$ is photon energy, $E_0$ is single oscillator energy, and $E_d$ is dispersion energy which is a measure of the average strength of interband optical transitions. Plotting refractive index factor $(n^2-1)^{-1}$ against $(h\nu)^2$ allows us to determine the oscillator parameters by fitting a straight line to the points, as shown in Fig. 4. It is worth emphasizing the goodness of the fits to the large wavelength experimental data. The values of WDD dispersion parameters, $E_0$ and $E_d$, for all thin films were directly determined from the slope

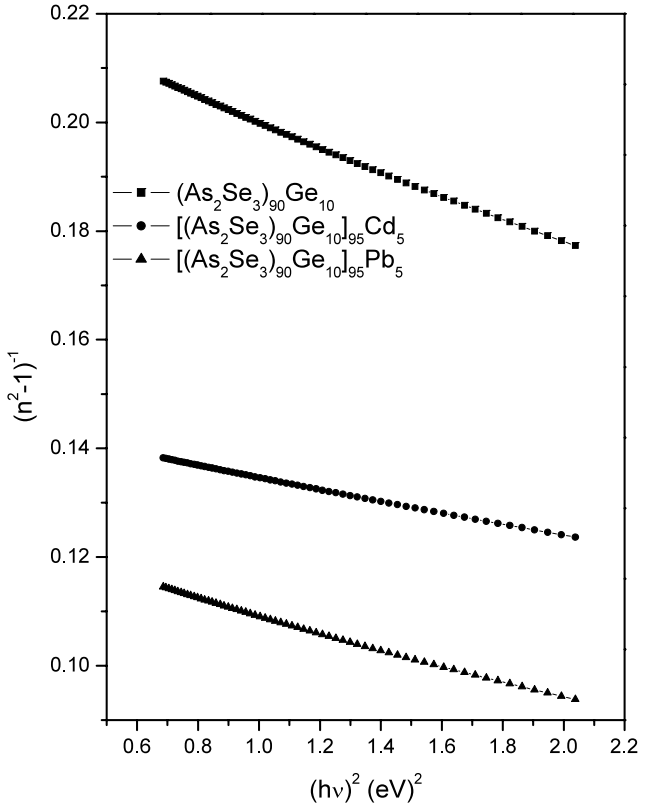


**Fig. 4** A plot of the refractive index factor $(n^2-1)^{-1}$ versus $(h\nu)^2$ for $a$-$[(As_2Se_3)_{90}Ge_{10}]_{95}M_5$ (where M = Cd and Pb) thin films

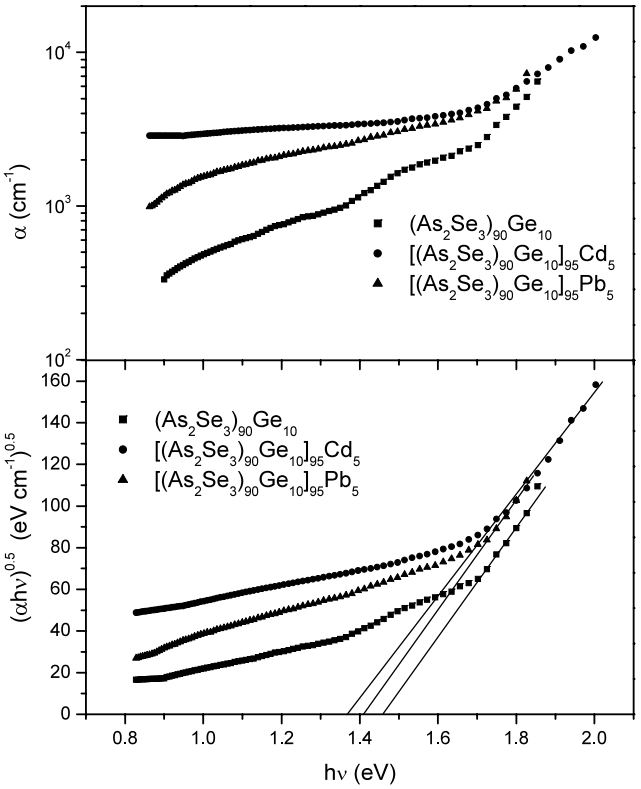


**Fig. 5** A plot of the absorption coefficient $(\alpha)$ and $(\alpha h\nu)^{1/2}$ versus $h\nu$ for $a$-$[(As_2Se_3)_{90}Ge_{10}]_{95}M_5$ (where M = Cd and Pb) thin films

$(E_0E_d)^{-1}$ and the intercept on the vertical axis $(E_0/E_d)$ of their corresponding least square straight lines. The values of these dispersion parameters are given in Table 1 for the thin films under investigation.

The values for the static refractive index $(n_0)$ have been calculated from WDD dispersion parameters $E_0$ and $E_d$ by using the formula

$$n_0 = \left(1 + \frac{E_d}{E_0}\right)^{1/2}. \tag{2}$$

The values of $n_0$ are calculated by extrapolating the WDD dispersion equation as $h\nu \to 0$. The values of $n_0$ are given in Table 1. The high frequency dielectric constant $(\varepsilon_\infty)$ has been calculated from the relation $\varepsilon_\infty = (n_0)^2$, and the obtained values are reported in Table 1.

The absorption coefficient $(\alpha)$ of $[(As_2Se_3)_{90}Ge_{10}]_{95}M_5$, where M = Cd and Pb, thin films has been calculated using the relation $\alpha = (1/d)\ln(1/X)$, where $X$ is the absorbance [17]. The variation of absorption coefficient with photon energy for thin films is shown in Fig. 5 using a semi-logarithmic scale. The optical energy gap has been estimated from absorption coefficient data as a function of wavelength by using the relation [23]

$$(\alpha h\nu)^{0.5} = B\left(h\nu - E_g^{\text{opt}}\right), \tag{3}$$

where $B$ is the slope of Tauc edge, called energy tailing parameter, that depends on the width of localized states in the energy gap which are attributed to homopolar bonds in chalcogenide glasses. This relationship allows us to estimate the value of optical energy gap. Figure 5 shows the plot of $(\alpha h\nu)^{0.5}$ against $h\nu$. The values of $E_g^{\text{opt}}$ can readily be calculated from the plot of $(\alpha h\nu)^{0.5}$ as a function of $h\nu$ by taking the intercept of the extrapolations to zero absorption with the photon energy axis as $(\alpha h\nu)^{0.5} \to 0$. The obtained values of $E_g^{\text{opt}}$ for indirect allowed transitions are given in Table 2.

Figure 6 shows the plot of dielectric constants (real and imaginary). The dielectric constant of $[(As_2Se_3)_{90}Ge_{10}]_{95}M_5$ thin films can be calculated with the help of refractive index $(n)$ and extinction coefficient $(k)$ [24]. The real dielectric constant $\varepsilon_r$ can be calculated from the relation $\varepsilon_r = n^2 - k^2$ and the imaginary dielectric constant $\varepsilon_i$ can be calculated from the following relation $\varepsilon_i = 2nk$. The variation of both real and imaginary dielectric with wavelength follows the same trend as that of refractive index and extinction coefficient. The optical parameters, i.e., $n$, $k$, $\varepsilon_r$, and $\varepsilon_i$, decrease with increasing wavelength. Figure 7 shows the variation of optical conductivity in terms of photon energy. The optical conductivity directly depends on the absorption coefficient and refractive index and has been determined from the relation [25] $\sigma = \alpha nc/4\pi$, where $c$ is the

**Table 2** The values of the optical energy gap ($E_g^{opt}$), real part of dielectric constant ($\varepsilon_r$), imaginary part of dielectric constant ($\varepsilon_i$), and the optical conductivity ($\sigma$) for $a$-$[(As_2Se_3)_{90}Ge_{10}]_{95}M_5$ (where M = Cd and Pb) thin films at 800 nm

| Composition | $E_g^{opt}$ (eV) | $\varepsilon_r$ | $\varepsilon_i$ | $\sigma$ ($s^{-1}$) |
|---|---|---|---|---|
| $(As_2Se_3)_{90}Ge_{10}$ | $1.46 \pm 0.01$ | 6.97 | 0.0621 | $1.2 \times 10^{13}$ |
| $[(As_2Se_3)_{90}Ge_{10}]_{95}Cd_5$ | $1.36 \pm 0.01$ | 9.328 | 0.1447 | $2.7 \times 10^{13}$ |
| $[(As_2Se_3)_{90}Ge_{10}]_{95}Pb_5$ | $1.41 \pm 0.01$ | 12.23 | 0.1389 | $2.6 \times 10^{13}$ |

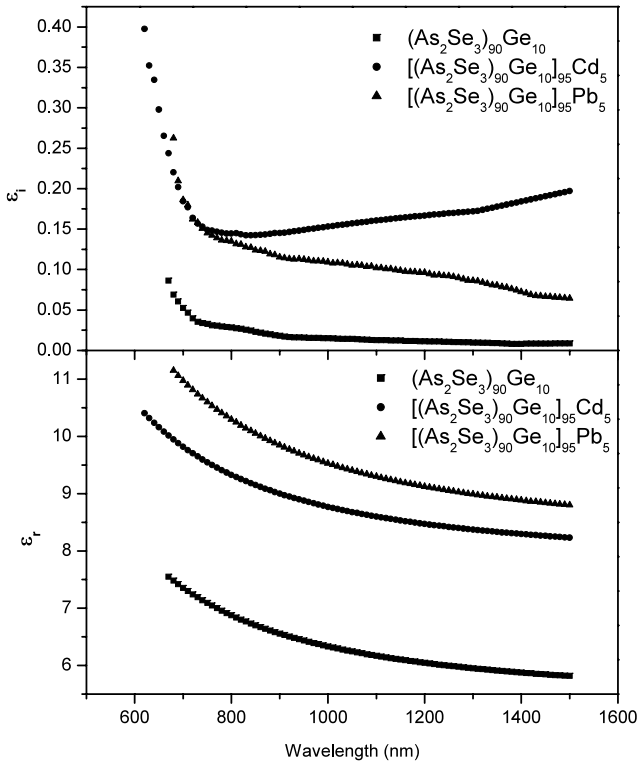


**Fig. 6** A plot of the real part ($\varepsilon_r$) and the imaginary part ($\varepsilon_i$) of the dielectric constant versus $h\nu$ for $a$-$[(As_2Se_3)_{90}Ge_{10}]_{95}M_5$ (where M = Cd and Pb) thin films

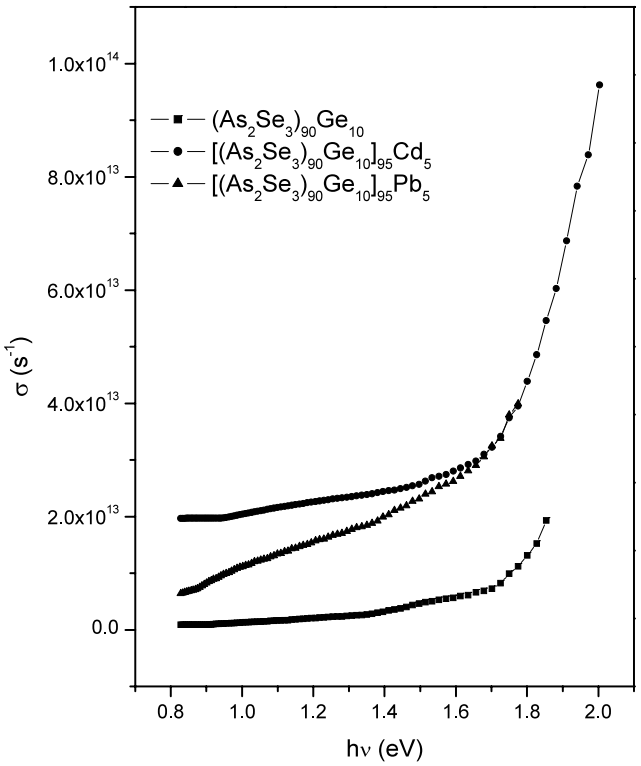


**Fig. 7** A plot of the optical conductivity ($\sigma$) versus $h\nu$ for $a$-$[(As_2Se_3)_{90}Ge_{10}]_{95}M_5$ (where M = Cd and Pb) thin films

velocity of light, $\alpha$ is the absorption coefficient, and $n$ is the refractive index.

## 4 Discussion

Figure 1 shows that transmission decreases significantly with the addition of metal impurities. Spectral distribution of refractive index in Fig. 2 inferred that both refractive index and extinction coefficient decrease with the increase of wavelength for thin films under investigation. The decrease in the value of refractive index with wavelength shows the normal dispersion behavior of the material. On the part of metal impurities addition to $(As_2Se_3)_{90}Ge_{10}$ thin films, the refractive index has been found to have higher values (Table 1). This increase in the refractive index may be ascribed to an increase in density (Table 1), change in stoichiometry and internal strain caused by the addition of metal impurities. The individual increase in different metal added thin films may be explained on the basis of polarizability. The larger the atomic radius of the atom, the larger will its polarizability be, and consequently, according to the Lorentz–Lorenz relation (4) between refractive index and polarizability, the larger will the refractive index be:

$$\frac{n^2-1}{n^2+2} = \frac{1}{3\varepsilon_0}\sum_i N_i\alpha_{pi}, \tag{4}$$

where $\varepsilon_0$ is the vacuum permittivity, $N_i$ is the number of polarizable units of type $i$ per unit volume with polarizability $\alpha_{pi}$. The atomic radii of Cd and Pb are 1.41 and 1.54 Å, respectively. It is clear from Table 1 that the refractive index follows the same trend as that of the atomic radii for

different impurity metals. The dispersion of refractive index (spectral dependence) has been analyzed in terms of the WDD model which is based on a single effective oscillator approach. The high frequency properties of thin films under investigation could be treated as those of a single oscillator. The calculated WDD parameters $E_0$ (also called the average energy gap) and $E_d$ are in good agreement with the earlier reported results [21, 22]. The values of $E_0$ decrease with the addition of metal impurities (Table 1). This may be due to the increase of density of states in the valence band. Nevertheless, it must be noted that the WDD model is only valid in transparent region where the absorption coefficient of chalcogenide thin films takes values $\alpha \approx 0$. The detailed analysis of the dispersion of refractive index, in terms of the WDD model, throws very valuable light on the structure of material through the values of the dispersion energy parameter $E_d$. The parameter $E_d$ is related to other physical parameters by the simple empirical relation proposed by WDD, i.e., $E_d = \beta N_c Z_a N_e$, where $\beta$ is a two-valued constant [22] with either an ionic or covalent value (for ionic materials $\beta = 0.26 \pm 0.03$ eV, and for covalent materials $\beta = 0.37 \pm 0.04$ eV), $N_c$ is the effective coordination number of cation nearest neighbor to anion, $N_e$ is the effective number of valence electrons per anion. Furthermore, it has been observed that the single oscillator parameter $E_0$ is in concord to the relation $E_0 \approx 2 \times E_g^{\text{opt}}$ obtained by Tanaka [26] when studying vitreous films having a composition $As_xS_{100-x}$, and which subsequently hold for other vitreous chalcogenide thin films [27, 28].

Analysis of the optical absorption spectra is one of the most productive tools for understanding and developing the energy band diagram of both crystalline and amorphous materials. It is well known that the optical gap of amorphous semiconducting alloys strongly depends on their composition. Optical absorption in solids or liquids can occur by several different mechanisms, all of which involve coupling of the electric field vector of the incident radiation to dipole moments in the material and hence a consequent transfer of energy. The excitation of electrons from filled to empty states by photon absorption is of primary importance in semiconductors. The onset of the optical absorption processes is marked by rise in the absorption coefficient ($\alpha$) over many decades, the fundamental absorption edge, to a level of $\approx 10^4$ cm$^{-1}$ at a photon energy corresponding to the energy gap. In crystals, the transition can be "direct" or "indirect", the later being phonon-assisted. The form of the edge depends on the symmetry of the wave functions and the effective masses of electrons and holes at the edges of the valence and conduction bands. In present study for freshly prepared thin films, there is no sharp increase in the absorption coefficient near the fundamental absorption edge, indicating an indirect energy transition in the forbidden gap [29]. The optical energy gap has been estimated by Tauc's extrapolation and found to decrease with the addition of metal impurities to $(As_2Se_3)_{90}Ge_{10}$ thin films. In the fundamental absorption region, the absorption is due to the transition from the top of valence band to the bottom of the conduction band. The addition of metal impurities in $(As_2Se_3)_{90}Ge_{10}$ thin films may cause an increase in the density of states in the valence band. The addition of metal impurities may also create localized states in the energy gap [30]. This will lead to a shift in the absorption edge towards lower photon energy, and consequently the decrease in the optical energy gap can be explained by the increased tailing of the conduction band edge into the gap.

Dielectric response of the materials, i.e., the variation of real, $\varepsilon_r$, and imaginary, $\varepsilon_i$, parts of the dielectric constant with wavelength is shown in Fig. 6. The complex dielectric constant is a fundamental intrinsic material property. The dielectric constant of a material affects the movement of electromagnetic signals through the material. A high value of the dielectric constant makes the distance inside the material look bigger. Thus, the light travels more slowly. In general, the real part of the dielectric constant is associated with the term that describes how much the material will slow down the speed of light, and the imaginary part explains how a dielectric absorbs energy from an electric field due to dipole motion. The knowledge of real and imaginary parts of the dielectric constant provides information about the loss factor which is the ratio of the imaginary part of the dielectric constant and the real part of the dielectric constant. The larger the imaginary part of the dielectric constant or the smaller the real part of the dielectric constant, the larger is the loss factor. It is clear from Fig. 6 that both real and imaginary dielectric constants decrease with the increase in wavelength. This may be due to the decrease of the absorption coefficient with the increase in wavelength. On the part of metal impurities, $\varepsilon_r$ and $\varepsilon_i$ follow the same trend as that of the refractive index and extinction coefficient.

The optical response of the material is most conveniently studied in terms of optical conductivity ($\sigma$). It has the dimensions of frequency which are valid only in Gaussian system of units. With the addition of metal impurities, the optical conductivity shifts towards the lower photon energy side. This may be due to the fact that optical conductivity directly depends on the absorption coefficient of the thin film. The optical conductivity has higher values for impurity-added thin films. This increase may be a consequence of the increased density of localized states in the gap itself due to the appearance of new defect states and Cd/Pb containing structural elements.

## 5 Conclusion

The effect of M = Cd and Pb on the optical properties of thermally evaporated amorphous $[(As_2Se_3)_{90}Ge_{10}]_{95}M_5$

thin films has been studied using normal incidence transmission spectra in the spectral range 400–1500 nm. The refractive index increases with the addition of metal impurities to $(As_2Se_3)_{90}Ge_{10}$ thin films, and is explained on the basis of increase in the polarizability. The dispersion of refractive index has been analyzed using Wemple–DiDomenico single oscillator model, and it is found that the dispersion parameter $E_0$ is in concordance with the Tanaka's relation. The transition in the energy gap has been found to be of indirect type and to decrease with the addition of metal impurities. This decrease in the optical energy gap has been explained on the basis of the increase in the density of states in the valence band. The dielectric constant and optical conductivity for metal added thin films have higher values.

## References


1. M. Frumar, B. Frumarova, P. Nemec, T. Wagner, J. Jedelsky, M. Hrdlicka, J. Non-Cryst. Solids **352**, 544 (2006)
2. N.P. Eisenberg, M. Manevich, A. Arsh, M. Klebanov, V. Lyubin, J. Non-Cryst. Solids **352**, 1632 (2006)
3. I.D. Aggarwal, J.S. Sanghera, J. Non-Cryst. Solids **256–257**, 6 (1999)
4. Q.M. Liu, F.X. Gan, X.J. Zhao, K. Tanaka, A. Narazaki, K. Hirao, Opt. Lett. **26**, 1347 (2001)
5. P. Sharma, S.C. Katyal, J. Phys. D, Appl. Phys. **40**, 2115 (2007)
6. R.P. Wang, A.V. Rode, S.J. Madden, C.J. Zha, R.A. Jarvis, B. Luther-Davies, J. Non-Cryst. Solids **353**, 950 (2007)
7. E. Skordeva, K. Christova, M. Tzolov, Z. Dimitrova, Appl. Phys. A **66**, 103 (1998)
8. Z.U. Borisova, *Glassy Semiconductors* (Plenum, New York, 1981)
9. H. Fritzsche, M. Kaster, Philos. Mag. B **37**, 285 (1978)
10. P. Sharma, S.C. Katyal, Mater. Lett. **61**, 4516 (2007)
11. M.M. El-Samanoudy, Thin Solid Films **423**, 201 (2003)
12. E. Bacaksiz, B.M. Basol, M. Altunbas, V. Novruzov, E. Yanmaz, S. Nezir, Thin Solid Films **515**, 3079 (2007)
13. P. Sharma, S.C. Katyal, Thin Solid Films **515**, 7966 (2007)
14. P. Sharma, S.C. Katyal, Philos. Mag. **88**, 2549 (2008)
15. A.K. Pattanaik, A. Srinivasan, Semicond. Sci. Technol. **19**, 157 (2004)
16. J.C. Manifacier, J. Gasiot, J.P. Fillard, J. Phys. E, Sci. Instrum. **9**, 1002 (1976)
17. R. Swanepoel, J. Phys. E, Sci. Instrum. **16**, 1214 (1983)
18. I. Sharma, S.K. Tripathi, P.B. Barman, J. Phys. D, Appl. Phys. **40**, 4460 (2007)
19. D.D. Strbac, S.R. Lukic, D.M. Petrovic, J.M. Gonzalez-Leal, A. Srinivasan, J. Non-Cryst. Solids **353**, 1466 (2007)
20. P. Sharma, S.C. Katyal, Physica B **403**, 3667 (2008)
21. S.H. Wemple, M. DiDomenico, Phys. Rev. B **3**, 1338 (1971)
22. S.H. Wemple, Phys. Rev. B **7**, 3767 (1973)
23. J. Tauc, *The Optical Properties of Solids* (North-Holland, Amsterdam, 1970)
24. A. Goswami, *Thin Film Fundamental* (New Age International, New Delhi, 2005)
25. J.I. Pankove, *Optical Processes in Semiconductors* (Dover, New York, 1975)
26. K. Tanaka, Thin Solid Films **66**, 271 (1980)
27. J.M. Gonzalez-Leal, A. Ledesma, A.M. Bernal-Oliva, R. Prieto-Alcon, E. Marquez, J.A. Angel, J. Carabe, Mater. Lett. **39**, 232 (1999)
28. T.I. Kosa, T. Wagner, P.J.S. Ewen, A.E. Owen, Philos. Mag. B **71**, 311 (1995)
29. Y.P. Venkata Subbaiah, P. Pratap, K.T.R. Reddy, D. Mangalaraj, K. Kim, Yi Junsin, J. Phys. D, Appl. Phys. **40**, 3683 (2007)
30. N. Barreau, S. Marsillac, J.C. Bernede, T. Ben Nasrallah, S. Belgacem, Phys. Stat. Sol. (a) **184**, 179 (2001)